Analytic Charge Model for Double-Gate and Surrounding-Gate MOSFETs

Bo Yu*, Huaxin Lu**, Wei-Yuan Lu* and Yuan Taur*

* Department of Electrical and Computer Engineering
University of California at San Diego, La Jolla, CA, USA
** Texas Instruments, Dallas, TX, USA

ABSTRACT

An analytic charge model for both double gate and surrounding gate MOSFETs is presented. With only the mobile charge term, Poisson's equation is rigorous solved and the analytic electrostatic potential is derived. The development of charge model is based on closed-form solution of Poisson's equation, current continuity equation, and Ward-Dutton linear charge partition. The model can continuously cover all the operation regions, i.e., linear, saturation, and subthreshold, with unique analytic expressions. The physics-based nature makes this model free of fitting parameters as well as the charge sheet approximation. It is shown that the C-V characteristics generated by this model agree with two-dimensional numerical simulation results.

Keywords: MOSFETs, modeling, double gate, surrounding gate.

1 INTRODUCTION

Double gate (DG) and surrounding gate (SG) MOSFETs have been proposed to scale down CMOS technology more aggressively [1], since bulk CMOS scaling [2], [3] is approaching the limit imposed by gate oxide tunnelling, body doping, and band-to-band tunneling, *etc.*. Efforts toward analytic model for these new device structures are presented in this paper, with emphasis on the charge model. Recently, continuous analytic drain current models have been developed for DG [4] and SG [5] MOSFETs, respectively. Without charge sheet approximation [6], these two models are derived directly from the Pao-Sah integral [7] for DG and SG MOSFETs with undoped or lightly doped silicon body. However, drain current model is not enough for circuit simulation [8]. Therefore, terminal charge models for both DG [9] and SG [10] MOSFETs have been proposed to calculate the dynamic behavior of the device and hence to enable AC and transient circuit simulation. The conventional Ward-Dutton charge partition method [11] for bulk MOSFETs can also be applied to define terminal charges for DG and SG MOSFETs. It has been validated by numerical simulations that these models can continuously cover all the three operation regions without the need for non-physical fitting parameters.

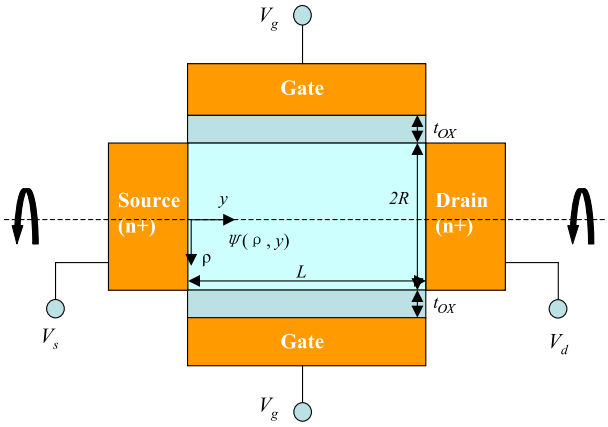

Figure 1: Schematic diagram of an SG MOSFET (cut through symmetry axis).

2 ANALYTIC CHARGE MODEL FOR SG MOSFETS

Consider an undoped (or lightly doped) cylindrical SG MOSFET schematically shown in Fig. 1. Under the gradual channel approximation, Poisson's equation takes the following form with only the mobile charge (electrons) term:

$$\frac{d^2\psi}{d\rho^2} + \frac{1}{\rho}\frac{d\psi}{d\rho} = \frac{q}{\epsilon_{si}} n_i e^{\frac{q(\psi - V)}{kT}} \tag{1}$$

where q is the electronic charge, ϵ_{si} is the permittivity of silicon, n_i is the intrinsic carrier density, $\psi(\rho)$ is the electrostatic potential, and V is the electron quasi-Fermi potential which is constant in the ρ-direction. Here we consider an nMOSFET with $q\psi/kT \gg 1$ so that the hole density is negligible.

The solution of Eq. (1) has been presented in a previous paper by Jimenez *et al.* [5]. We reorganize it as

$$\psi(\rho) = V - \frac{2kT}{q} \ln\left[\frac{R}{2L_{Di}} \frac{1}{\sqrt{1-\alpha}} \left(1 - \frac{(1-\alpha)\rho^2}{R^2}\right)\right] \tag{2}$$

where $L_{Di} = \sqrt{2\epsilon_{si}kT/q^2 n_i}$ is the intrinsic Debye length, and α is to be determined by the boundary condition

NSTI-Nanotech 2007, www.nsti.org, ISBN 1420061844 Vol. 3, 2007

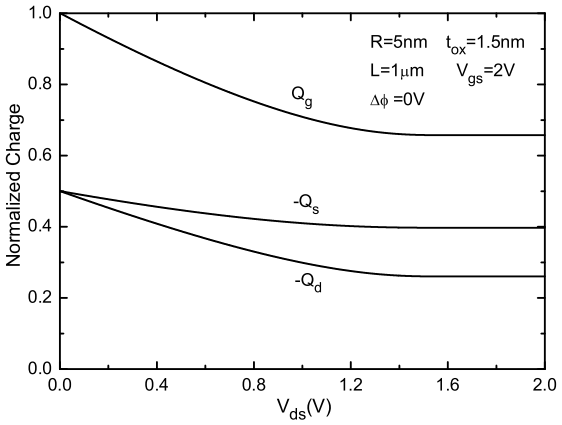

Figure 2: Normalized terminal charges Q_g, Q_s, and Q_d of an SG MOSFET as functions of V_{ds}. The normalization constant is $8\pi\epsilon_{si}L\left(kT/q\right)\left(1-\alpha_s\right)/\alpha_s$.

which has final form as

$$\frac{1}{2}\ln\left(1-\alpha\right)-\ln\alpha+s\frac{1-\alpha}{\alpha} = \frac{q\left(V_g-\Delta\phi-V\right)}{2kT}-\ln\left(\frac{2L_{Di}}{R}\right). \quad (3)$$

Here $s=2\epsilon_{si}\ln(1+\frac{t_{ox}}{R})/\epsilon_{ox}$ is a structural parameter, ϵ_{ox} is the permittivity of oxide, V_g is the voltage applied to the gate, R is the radius of silicon cylinder, t_{ox} is the oxide thickness, and $\Delta\phi$ is the work function of gate electrode with respect to the intrinsic silicon. The range of α is $0<\alpha<1$. Because (3) is an implicit equation of α, the general approach to solve α is Newton-Ralphson numerical method.

From Gauss's law, the total mobile charge per unit gate area $Q_i=2\epsilon_{si}(2kT/q)(1-\alpha)/\alpha/R$. $dV/d\alpha$ can also be expressed as a function of α by differentiating (3): $dV/d\alpha=(kT/q)[1/(1-\alpha)+2/\alpha+2s/\alpha^2]$. Therefore, the drain current can be calculated as

$$\begin{aligned} I_{ds} &= \mu\frac{2\pi R}{L}\int_{V_s}^{V_d}Q_i(V)dV \\ &= \mu\frac{2\pi R}{L}\int_{\alpha_s}^{\alpha_d}Q_i(\alpha)\frac{dV}{d\alpha}d\alpha \\ &= \mu\frac{8\pi\epsilon_{si}}{L}\left(\frac{kT}{q}\right)^2\left[f\left(\alpha_d\right)-f\left(\alpha_s\right)\right] \end{aligned} \quad (4)$$

where μ is the effective mobility, L is the channel length, V_s, V_d are the voltages applied to the source and drain, respectively, α_s, α_d are solutions to (3) corresponding to $V=V_s$ and $V=V_d$, respectively, and $f(\alpha)=(-2/\alpha-\ln\alpha)+s\left(-1/\alpha^2+2/\alpha\right)$.

Analytic expressions for three terminal charges, i.e., Q_g, Q_s, and Q_d, associated with gate, source, and drain, respectively, are required for circuit simulation of SG MOSFETs. The gate charge can be computed directly by integrating the charge density along the channel. For the source and drain charges, it is physically sound to adopt Ward-Dutton linear charge partition method, which is widely accepted for bulk MOSFETs [11]. Integrating the current continuity equation

$$dy=\mu(2\pi R)Q_i dV/I_{ds} \quad (5)$$

leads to $y=L[f(\alpha)-f(\alpha_s)]/[f(\alpha_d)-f(\alpha_s)]$. With this result, we can calculate the terminal charges as

$$\begin{aligned} Q_g &= 2\pi R\int_0^L Q_i(y)dy \\ &= \left(2\pi R\right)^2\frac{\mu}{I_{ds}}\int_{\alpha_s}^{\alpha_d}Q_i^2(\alpha)\frac{dV}{d\alpha}d\alpha \\ &= 8\pi\epsilon_{si}L\frac{kT}{q}\frac{g\left(\alpha_d\right)-g\left(\alpha_s\right)}{f\left(\alpha_d\right)-f\left(\alpha_s\right)} \\ Q_d &= -2\pi R\int_0^L\frac{y}{L}Q_i(y)dy=8\pi\epsilon_{si}L\frac{kT}{q}W_{sd} \\ Q_s &= -2\pi R\int_0^L\left(1-\frac{y}{L}\right)Q_i(y)dy=8\pi\epsilon_{si}L\frac{kT}{q}W_{ds} \end{aligned} \quad (6)$$

where

$$W_{ij}=\frac{f\left(\alpha_i\right)\left[g\left(\alpha_j\right)-g\left(\alpha_i\right)\right]+\left[h\left(\alpha_j\right)-h\left(\alpha_i\right)\right]}{\left[f\left(\alpha_j\right)-f\left(\alpha_i\right)\right]^2} \quad (7)$$

and functions $g(\alpha)$ and $h(\alpha)$ are defined as

$$\begin{aligned} g\left(\alpha\right) &= \left(-\frac{1}{\alpha^2}+\frac{3}{\alpha}+\ln\alpha\right)+s\left(-\frac{2}{3\alpha^3}+\frac{2}{\alpha^2}-\frac{2}{\alpha}\right) \\ h\left(\alpha\right) &= \left(-\frac{4}{3\alpha^3}+\frac{5}{2\alpha^2}+\frac{1}{\alpha}-\frac{1-3\alpha}{\alpha^2}\ln\alpha+\frac{\left(\ln\alpha\right)^2}{2}\right) \\ &\quad -s\left(\frac{3}{2\alpha^4}-\frac{43}{9\alpha^3}+\frac{9}{2\alpha^2}+\frac{2-6\alpha+6\alpha^2}{3\alpha^3}\ln\alpha\right) \\ &\quad -s^2\left(\frac{2}{5\alpha^5}-\frac{2}{\alpha^4}+\frac{10}{3\alpha^3}-\frac{2}{\alpha^2}\right). \end{aligned} \quad (8)$$

The imaginary component of the small-signal behavior of a three-terminal device can be characterized by nine nonreciprocal capacitance coefficients. Here, we shall adopt the convention in which the capacitance coefficient C_{mn} is defined as $\delta_{mn}\times\partial Q_m/\partial V_n$, where $m,n=g,s,d$, and δ_{mn} is equal to 1 if $m=n$, and -1 if otherwise. For simplicity, we will only list the results of four linearly independent components, from which all

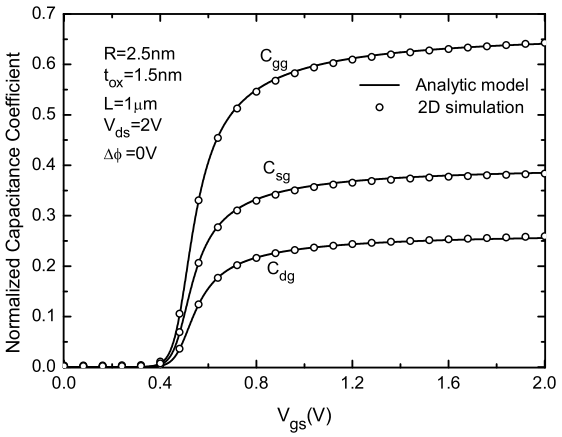

Figure 3: Normalized capacitance coefficients of an SG MOSFET as functions of V_{gs} obtained from the analytic model (solid lines), in comparison with the 2-D numerical simulation results (open circles). The normalization constant is $4\pi\epsilon_{si}L/s$ ($V_{ds} = 2V$).

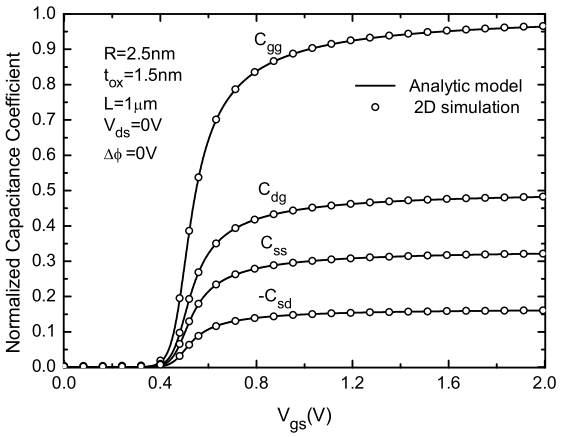

Figure 4: Normalized capacitance coefficients of an SG MOSFET as functions of V_{gs} obtained from the analytic model (solid lines), in comparison with the 2-D numerical simulation results (open circles). The normalization constant is $4\pi\epsilon_{si}L/s$ ($V_{ds} = 0V$).

the nine capacitance coefficients can be obtained directly based on the charge conservation law [8]:

$$\begin{aligned}
C_{gs} &= \frac{L^2\left(g_{ds}+g_m\right)^2}{\mu I_{ds}} - \frac{Q_g\left(g_{ds}+g_m\right)}{I_{ds}} \\
&= 8\pi\epsilon_{si}L\frac{1-\alpha_s}{\alpha_s}\frac{\left[\left(1-\alpha_s\right)/\alpha_s + W_{sd} + W_{ds}\right]}{f\left(\alpha_d\right)-f\left(\alpha_s\right)} \\
C_{gd} &= -\frac{L^2 g_{ds}^2}{\mu I_{ds}} + \frac{Q_g g_{ds}}{I_{ds}} \\
&= 8\pi\epsilon_{si}L\frac{1-\alpha_d}{\alpha_d}\frac{\left[\left(1-\alpha_d\right)/\alpha_d + W_{sd} + W_{ds}\right]}{f\left(\alpha_s\right)-f\left(\alpha_d\right)} \\
C_{dg} &= -\frac{L^2 g_{ds}^2}{\mu I_{ds}} + \frac{Q_g g_{ds}}{I_{ds}} - \frac{\left(Q_s-Q_d\right)g_m}{I_{ds}} \\
&= 8\pi\epsilon_{si}L\{\frac{1-\alpha_d}{\alpha_d}\frac{\left[\left(1-\alpha_d\right)/\alpha_d + W_{sd} + W_{ds}\right]}{f\left(\alpha_s\right)-f\left(\alpha_d\right)} \\
&\qquad + \left(W_{ds}-W_{sd}\right)\frac{1/\alpha_s - 1/\alpha_d}{f\left(\alpha_s\right)-f\left(\alpha_d\right)}\} \\
C_{sd} &= \frac{\left(Q_s-Q_d\right)g_{ds}}{I_{ds}} \\
&= 8\pi\epsilon_{si}L\frac{1-\alpha_d}{\alpha_d}\frac{\left(W_{ds}-W_{sd}\right)}{f\left(\alpha_d\right)-f\left(\alpha_s\right)}. \qquad (9)
\end{aligned}$$

Here transconductance g_m and conductance g_{ds} are given by

$$\begin{aligned}
g_m &= \left.\frac{\partial I_{ds}}{\partial V_{gs}}\right|_{V_{ds}} = \mu\frac{8\pi\epsilon_{si}}{L}\frac{kT}{q}\left(\frac{1}{\alpha_s}-\frac{1}{\alpha_d}\right) \\
g_{ds} &= \left.\frac{\partial I_{ds}}{\partial V_{ds}}\right|_{V_{gs}} = \mu\frac{8\pi\epsilon_{si}}{L}\frac{kT}{q}\frac{1-\alpha_d}{\alpha_d} \qquad (10)
\end{aligned}$$

where $V_{gs} = V_g - V_s$ and $V_{ds} = V_d - V_s$. It is worthy to mention that this model is non-source-referenced and automatically preserves the symmetry with respect to source-drain interchange. This property can be obviously observed in the final expressions of the terminal charges as well as the capacitance coefficients.

All these analytic expressions have infinite order of continuity, however, they become the form 0/0, i.e., both the numerator and denominator are 0, when $V_s = V_d$. Inasmuch as the indeterminacies of type 0/0 will cause problems in numerical implementation, we have to provide expressions for the exact values at $V_s = V_d$, which are the limits of general expressions as V_d approaches V_s. These limits can be calculated through L'Hospital's rule or Taylor expansion. After a lengthy derivation, we finally obtain the results as

$$Q_g = -2Q_s = -2Q_d = 8\pi\epsilon_{si}L\frac{kT}{q}\frac{1-\alpha_s}{\alpha_s} \qquad (11)$$

$$\begin{aligned}
C_{gg} &= 2C_{gs} = 2C_{gd} = 2C_{sg} = 2C_{dg} = -6C_{sd} = -6C_{ds} \\
&= 3C_{ss} = 3C_{dd} = 8\pi\epsilon_{si}L\frac{1-\alpha_s}{2\alpha_s - \alpha_s^2 + 2s\left(1-\alpha_s\right)}. \qquad (12)
\end{aligned}$$

Fig. 2 plots terminal charges as functions of drain voltage. In this case, α_s is small. When $V_{ds} = 0$, $Q_g = -2Q_s = -2Q_d \simeq 8\pi\epsilon_{si}LkT/q\alpha_s$. When the device enters saturation region, $Q_g \simeq -10Q_s/6 \simeq -10Q_d/4 \simeq 10\left(8\pi\epsilon_{si}LkT/q\alpha_s\right)/15$ according to (6). These approximate relations are exactly the same with those for bulk MOSFETs [8], and are clearly reflected in Fig. 2.

In Fig. 3, 4, and 5, we have compared our capacitance coefficient model with numerical simulation re-

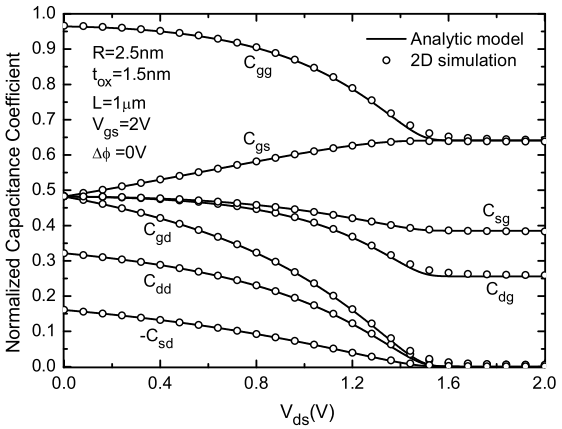

Figure 5: Normalized capacitance coefficients of an SG MOSFET as functions of V_{ds} obtained from the analytic model (solid lines), in comparison with the 2-D numerical simulation results (open circles). The normalization constant is $4\pi\epsilon_{si}L/s$.

sults of a long channel SG MOSFET. Because we use cylindrical coordinate instead of Cartesian coordinate, the numerical simulation is essentially two-dimensional. Fig. 3, where $V_{ds} = 2V$, shows that the general expressions of the model are in complete agreement with numerical simulations. In this case, the device is always in saturation region, and it is reasonable to assume $\alpha_d = 1$. Under this approximation, we can easily obtain the simple relation between capacitance coefficients from (9): $C_{gg} = C_{gs}$, $C_{sg} = C_{ss}$, $C_{dg} = -C_{ds}$, and $C_{gd} = C_{sd} = C_{dd} = 0$. If we further consider the well-above threshold region, where α_s is small, we can even derive the simplified approximate expressions for these capacitance coefficients as follow

$$C_{gg} \simeq \frac{10}{6}C_{sg} \simeq \frac{10}{4}C_{dg} \simeq \frac{10}{15}\frac{4\pi\epsilon_{si}L}{s}\left(1-\frac{\alpha_s}{s}\right). \qquad (13)$$

Fig. 4 indicates the validity of (12) for the special case of $V_s = V_d$. In Fig. 5, the capacitance coefficients from both analytic model and numerical simulation are compared as functions of V_{ds}. We can clearly observe the transition between two degenerate cases, which have been introduced above: one degeneracy is from source-drain-interchange symmetry at $V_{ds} = 0$; another is induced by saturation at the drain end.

3 ANALYTIC CHARGE MODEL FOR DG MOSFETS

Consider an undoped (or lightly doped) symmetric DG MOSFET schematically shown in Fig. 6. Under the gradual channel approximation, Poisson's equation

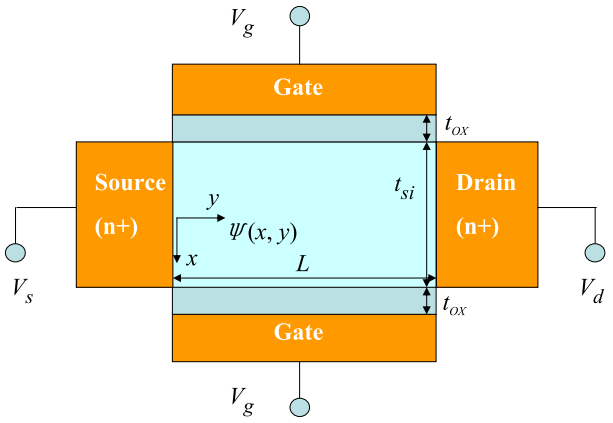

Figure 6: Schematic diagram of an DG MOSFET (no dependence on the third direction).

takes the following form with only the mobile charge (electrons) term:

$$\frac{d^2\psi}{dx^2} = \frac{q}{\epsilon_{si}}n_i e^{\frac{q(\psi-V)}{kT}} \qquad (14)$$

where $\psi(x)$ is the electrostatic potential, and V is the electron quasi-Fermi potential which is constant in the x-direction.

The solution of Eq. (14) has been presented in our previous paper [4] as

$$\psi(x) = V - \frac{2kT}{q}\ln\left[\frac{t_{si}}{2L_{Di}\beta}\cos\left(\frac{2\beta x}{t_{si}}\right)\right] \qquad (15)$$

where β is to be determined by the boundary condition which has final form as

$$\ln\beta - \ln(\cos\beta) + r\beta\tan\beta = \frac{q(V_g - \Delta\phi - V)}{2kT} - \ln\left(\frac{2L_{Di}}{t_{si}}\right). \qquad (16)$$

Here $r = 2\epsilon_{si}t_{ox}/\epsilon_{ox}t_{si}$ is a structural parameter, t_{si} is the silicon thickness. The range of β is $0 < \beta < \pi/2$. Because (16) is an implicit equation of β, the general approach to solve β is Newton-Ralphson numerical method.

Similarly, the drain current of DG MOSFET can be calculated as

$$I_{ds} = \mu\frac{8\epsilon_{si}}{L}\frac{W}{t_{si}}\left(\frac{kT}{q}\right)^2[p(\beta_d) - p(\beta_s)] \qquad (17)$$

where β_s, β_d are solutions to (16) corresponding to $V = V_s$ and $V = V_d$, respectively, and $p(\beta) = -2\beta\tan\beta + \beta^2 - r\beta^2\tan^2\beta$.

Analytic expressions for three terminal charges, i.e., Q_g, Q_s, and Q_d, associated with gate, source, and drain, respectively, are required for circuit simulation of DG

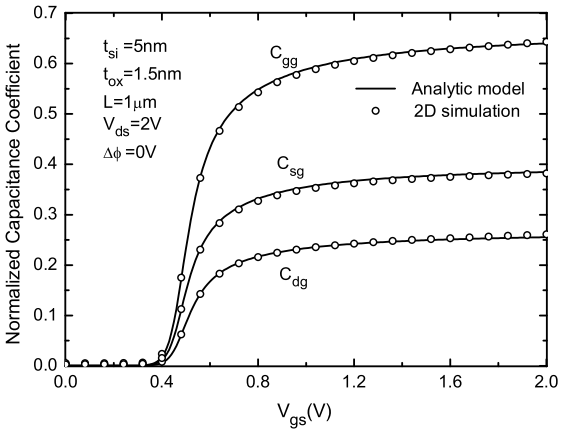

Figure 7: Normalized capacitance coefficients of an DG MOSFET as functions of V_{gs} obtained from the analytic model (solid lines), in comparison with the 2-D numerical simulation results (open circles). The normalization constant is $(4\epsilon_{si}L/r)(W/t_{si})$ $(V_{ds} = 2V)$.

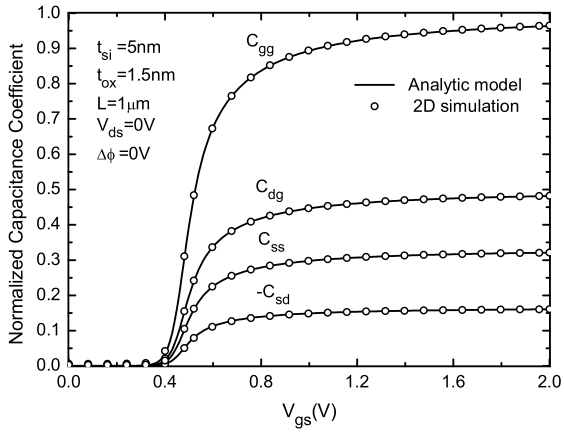

Figure 8: Normalized capacitance coefficients of an DG MOSFET as functions of V_{gs} obtained from the analytic model (solid lines), in comparison with the 2-D numerical simulation results (open circles). The normalization constant is $(4\epsilon_{si}L/r)(W/t_{si})$ $(V_{ds} = 0V)$.

MOSFETs. Following the Ward-Dutton linear charge partition, we can calculate the terminal charges as

$$\begin{aligned} Q_g &= 8\epsilon_{si}L\frac{W}{t_{si}}\frac{kT}{q}\frac{u(\beta_d)-u(\beta_s)}{p(\beta_d)-p(\beta_s)} \\ Q_d &= 8\epsilon_{si}L\frac{W}{t_{si}}\frac{kT}{q}U_{sd} \\ Q_s &= 8\epsilon_{si}L\frac{W}{t_{si}}\frac{kT}{q}U_{ds} \end{aligned} \tag{18}$$

where

$$U_{ij} = \frac{p(\beta_i)\left[u(\beta_j)-u(\beta_i)\right]+\left[v(\beta_j)-v(\beta_i)\right]}{\left[p(\beta_j)-p(\beta_i)\right]^2} \tag{19}$$

and functions $u(\beta)$ and $v(\beta)$ are defined as

$$\begin{aligned} u(\beta) &= -2\int_0^\beta \beta^2\tan^2\beta\left(\frac{1}{\beta}+\tan\beta\right)d\beta - \frac{2}{3}r\beta^3\tan^3\beta \\ v(\beta) &= 2\int_0^\beta \beta^2\tan^2\beta\left(\frac{1}{\beta}+\tan\beta\right)\left(\beta^2-2\beta\tan\beta\right)d\beta \\ &\quad - 2r\int_0^\beta \beta^4\tan^4\beta\left(\frac{1}{\beta}+\tan\beta\right)d\beta \\ &\quad + 2r\int_0^\beta \beta^2\tan^2\beta\left(\frac{\beta}{\cos^2\beta}+\tan\beta\right) \\ &\quad \times\left(\beta^2-2\beta\tan\beta\right)d\beta - \frac{2}{5}r^2\beta^5\tan^5\beta. \end{aligned} \tag{20}$$

It is straightforward to obtain expressions for conductance and transconductance

$$\begin{aligned} g_m &= \mu\frac{8\epsilon_{si}}{L}\frac{W}{t_{si}}\frac{kT}{q}\left(\beta_s\tan\beta_s-\beta_d\tan\beta_d\right) \\ g_{ds} &= \mu\frac{8\epsilon_{si}}{L}\frac{W}{t_{si}}\frac{kT}{q}\beta_d\tan\beta_d. \end{aligned} \tag{21}$$

Combining above results, we can finally derive the capacitance coefficients as follows

$$\begin{aligned} C_{gs} &= 8\epsilon_{si}L\frac{W}{t_{si}}\beta_s\tan\beta_s\frac{(\beta_s\tan\beta_s+U_{sd}+U_{ds})}{p(\beta_d)-p(\beta_s)} \\ C_{sd} &= 8\epsilon_{si}L\frac{W}{t_{si}}\beta_d\tan\beta_d\frac{(U_{ds}-U_{sd})}{p(\beta_d)-p(\beta_s)}. \end{aligned} \tag{22}$$

Here, we only list the results of two components, because all the other capacitance coefficients can be easily obtained based on source-drain interchange symmetry and charge conservation law.

When $V_s = V_d$, specific expressions are needed to avoid numerical instability:

$$Q_g = -2Q_s = -2Q_d = 8\epsilon_{si}L\frac{W}{t_{si}}\frac{kT}{q}\beta_s\tan\beta_s \tag{23}$$

$$\begin{aligned} C_{gg} &= 2C_{gs} = 2C_{gd} = 2C_{sg} = 2C_{dg} \\ &= -6C_{sd} = -6C_{ds} = 3C_{ss} = 3C_{dd} \\ &= 8\epsilon_{si}L\frac{W}{t_{si}}\frac{\frac{\beta_s}{\cos^2\beta_s}+\tan\beta_s}{2\left(\frac{1}{\beta_s}+\tan\beta_s\right)+2r\left(\frac{\beta_s}{\cos^2\beta_s}+\tan\beta_s\right)}. \end{aligned} \tag{24}$$

NSTI-Nanotech 2007, www.nsti.org, ISBN 1420061844 Vol. 3, 2007

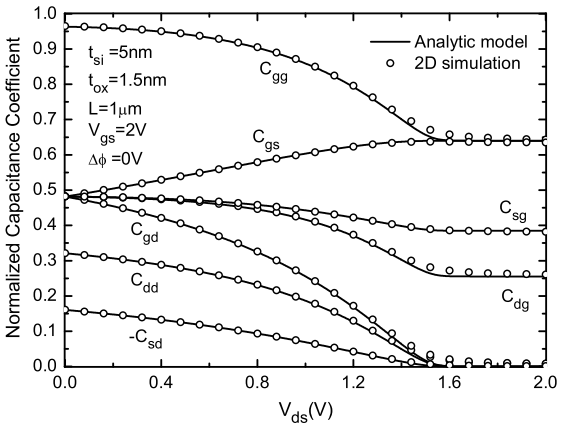

Figure 9: Normalized capacitance coefficients of an DG MOSFET as functions of V_{ds} obtained from the analytic model (solid lines), in comparison with the 2-D numerical simulation results (open circles). The normalization constant is $(4\epsilon_{si}L/r)(W/t_{si})$.

In Fig. 7, 8, and 9, we have compared our capacitance coefficient model with numerical simulation results of a long channel DG MOSFET. Fig. 7, where $V_{ds} = 2V$, shows that the general expressions of the model are in complete agreement with numerical simulations. In this case, the device is always in saturation region, and it is reasonable to assume $\beta_d = 0$. Under this approximation, we can easily obtain the simple relation between capacitance coefficients from (22): $C_{gg} = C_{gs}$, $C_{sg} = C_{ss}$, $C_{dg} = -C_{ds}$, and $C_{gd} = C_{sd} = C_{dd} = 0$. If we further consider the well-above threshold region, where $\beta_s \approx \pi/2$, we can even derive the simplified approximate expressions for these capacitance coefficients as follow

$$C_{gg} \simeq \frac{10}{6}C_{sg} \simeq \frac{10}{4}C_{dg} \simeq \frac{10}{15}\frac{4\epsilon_{si}L}{r}\frac{W}{t_{si}}\left(1 - \frac{1}{r\beta_s \tan\beta_s}\right) \tag{25}$$

Fig. 8 indicates the validity of (24) for the special case of $V_s = V_d$. In Fig. 9, the capacitance coefficients from both analytic model and numerical simulation are compared as functions of V_{ds}. We can clearly observe the transition between two degenerate cases.

4 CONCLUSION

In conclusion, we have presented an analytic charge model for both DG and SG MOSFETs. The model is non-source-referenced and preserves the source-drain symmetry inherently. Inasmuch as the essential physics has been preserved, it has been verified by numerical simulations that charge and capacitance coefficient behaviors in all the operation and transition regions are properly described by continuous functions without ad hoc fitting parameters. For SG MOSFETs, these continuous functions are simply composed of fundamental functions, making it suitable and easy to implement this predictive model in circuit simulation programs. However, for DG MOSFETs, because non-integrable functions are involved, table lookup method has to be employed to calculate terminal charges [9]. Therefore, we are aiming at improving the computational efficiency by making additional approximations. An optimal result is expected in the trade-off between efficiency and accuracy of the model [12].

REFERENCES

[1] J.-P. Colinge, "Multiple gate SOI MOSFETs," *Solid-State Electron.*, vol. 48, pp. 897-905, 2004.

[2] D.J. Frank, R. H. Dennard, E. Nowak, P. M. Solomon, Y. Taur, and H.-S. P.Wong, "Device scaling limits of Si MOSFETs and their application dependencies," *Proc. IEEE*, vol. 89, pp. 259-288, 2001.

[3] M. Liu, M. Cai, B. Yu, and Y. Taur, "Effect of gate overlap and source/drain doping gradient on 10-nm CMOS performance," *IEEE Trans. Electron Devices*, vol. 53, pp. 3146-3149, 2006.

[4] Y. Taur, X. Liang, W. Wang, and H. Lu, "A continuous, analytic drain-current model for DG MOSFETs," *IEEE Electron Device Lett.*, vol. 25, pp. 107-109, 2004.

[5] D. Jimenez, B. Iniguez, J. Sune, L. F. Marsal, J. Pallares, J Roig, and D. Flores, "Continuous analytic I-V model for surrounding-gate MOSFETs," *IEEE Electron Device Lett.*, vol. 25, pp. 571-573, 2004.

[6] J. R. Brews, "A charge sheet model of the MOSFET," *Solid-State Electron.*, vol. 21, pp. 345-355, 1978.

[7] H. C. Pao and C. T. Sah, "Effects of diffusion current on characteritics of metal-oxide (insulator)-semiconductor transistors," *Solid-State Electron.*, vol. 9, pp. 927-937, 1966.

[8] Y. Tsividis, *Operation and Modeling of the MOS Transistor*. Boston, MA: WCB/McGraw-Hill, 1999.

[9] H. Lu and Y. Taur, "An analytic potential model for symmetric and asymmetric double gate MOSFETs," *IEEE Trans. Electron Devices*, vol. 53, pp. 1161-1168, 2006.

[10] B. Yu, W.-Y. Lu, H. Lu, and Y. Taur, "Analytic Charge Model for Surrounding-Gate MOSFETs," *IEEE Trans. Electron Devices*, vol. 54, pp. 492-496, 2007.

[11] D. E. Ward and R. W. Dutton, "A charge-oriented model for MOS transistor capacitances," *IEEE J. Solid State Circuits*, vol. 13, pp. 703-708, 1978.

[12] H. Lu, "Compact modeling of Double-Gate MOSFETs," *Ph.D. thesis*, 2007.